Narrow-Band Blue Emitting Nitridomagnesosilicate Phosphor $Sr_8Mg_7Si_9N_{22}:Eu^{2+}$ for phosphor-converted LEDs

Chao Li,[a] Hong-Wei Zheng,[a] Heng-Wei Wei,[a] Jie Su,[b] Fu-Hui Liao,[b] Zhen-Yi Zhang,[c] Ling Xu,[a] Zu-Pei Yang,[ad] Xiao-Ming Wang,*[a] and Huan Jiao*[a]

Electronic Supplementary Information (ESI):

Experimental Section.

Sample Preparation. The compound $Sr_8Mg_7Si_9N_{22}$was prepared by solid state reactions in a horizontal tube furnace using the starting materials Sr_3N_2 (AR), amorphous Si_3N_4 (Alfa 95%), Mg powder (AR). EuF_2 (Alfa 99.5%). The raw materials were mixed in an agate mortar and filled into a tungsten crucible under argon atmosphere in a glovebox (Mikrouna, O_2 < 1 ppm, H_2O < 1 ppm). The tungsten crucible was placed in an alumina tube furnace and heated to 1400 °C with a rate of 300 °C/h and maintained at that temperature for 5h, and then followed by cooling down to 800 °C at a rate 1 °C/min. After reaction, the furnace down to room temperature spontaneously with power switch off and the tungsten crucible were opened in glovebox. All the heating and cooling processes are conducted in a reductive atmosphere of 6:94 (volume) H_2/N_2.

Single Crystal X-ray Diffraction. Single crystals were collected under a polarization microscope. The $Sr_8Mg_7Si_9N_{22}$ crystal data was collected using a Bruker D8 Quest diffractometer with PHOTON 100 CMOS detector and monochromatic Mo Kα radiation (λ = 0.71073 Å). A multiscan absorption correction was applied to the intensity datasets. The crystal structures were solved by Direct Methods (SHELXS) and refined by full-matrix least-squares methods (SHELXL).

High Resolution Powder X-ray Diffraction. In order to avoid hydrolysis, data were obtained using a PANalytical Empyrean diffractometer in capillary mode (Debye–Scherrer geometry using a Cu Kα radiation source (λ = 1.5418 Å) with a 0.5 mm borosilicate capillary sample holder at a spinning rate of 0.5 r/s to suppress the preferred orientation of the crystals) at 40 kV and 40 mA. The scan 2θ range was from 10° to 120° with a step size of 0.013° and a total data collection time of 3 h. The Rietveld refinements on X-ray diffraction data were performed by using the software TOPAS 5.

Density Functional Theory (DFT) Calculation. The DFT calculation of $Sr_8Mg_7Si_9N_{22}$ was performed with the Cambridge Serial Total Energy Package (CASTEP) code, in which plane wave basis set was chosen for the expansion of valance–electron wave functions at the local density approximation (LDA) level. There are two steps of calculations to obtain the electronic band structure of $Sr_8Mg_7Si_9N_{22}$. The first step was to optimize its crystal structure beginning with the crystallographic data refined from the XRD data by the Broyden–Fletcher–Goldfarb–Shannon (BFGS) method. In order avoid calculation error, the co-occupied Si2 and Mg3 were separated by reducing the space group symmetry to P1 (No.1). The second step was to calculate the band structure and density of states (DOS). For the calculations, energy cutoff of plane wave basis set was selected as 340 eV, and *K* -point sampling was chosen as 4 × 4 × 2 Monkhorst-Pack grid (separation ~0.04 $Å^{-1}$). Criterion for

the self-consistent field (SCF) was eigenenergy convergence within 1.0×10^{-7} eV/atom. Pseudopotential of each atom was constructed from the CASTEP database.

Scanning Electron Microscopy. The particle morphology of $Sr_8Mg_7Si_9N_{22}$ powder was observed by a scanning electron microscopy (SEM, FEI Q25) with an accelerating voltage of 20 kV. Chemical analysis were performed on energy dispersive X-ray spectroscopy (EDX) (EDAX, Element System) with an element silicon drift detector (SDD) and APEX™ software.

Luminescence Properties. The diffuse reflection spectrum was collected by a UV-3100 UV-vis-NIR spectrometer (Shimadzu, Japan) using the white powder $BaSO_4$ as a standard material. The photoluminescence emission and excitation spectra were measured at room temperature using a Hitachi F-4600 fluorescent spectrophotometer (Japan) with a 150 W Xe lamp as excitation source. The spectrum correction was applied and color coordinates were calculated by using the spectra data. High temperature PL spectra were investigated between 25 °C and 250 °C by using a TAP-02 high-temperature fluorescence analyzer. The luminescence decay curves were obtained by using a life time and steady state spectrometer (FLS920, Edinburgh Instruments Ltd). Absolute quantum efficiency was measured by the integrating sphere on the Edinburgh FLS 920 fluorescence spectrometer combined with a 450 W Xe lamp as the excitation source, and white $BaSO_4$ is employed to be a reference.

Band Gap Calculation from UV/vis Spectroscopy. The band gap is estimated according to Equation (1).

$$(\alpha h\nu)^n = A(h\nu - E_g) \qquad (1)$$

The hν is incident photon energy; A is a constant; α is the absorption coefficient; n = 2 for a direct transition or 1/2 for an indirect transition. The values of $(\alpha h\nu)^{1/2}$ are plotted as a function of the incident photon energy (hν) from the linear extrapolation of $(\alpha h\nu)^{1/2} = 0$.

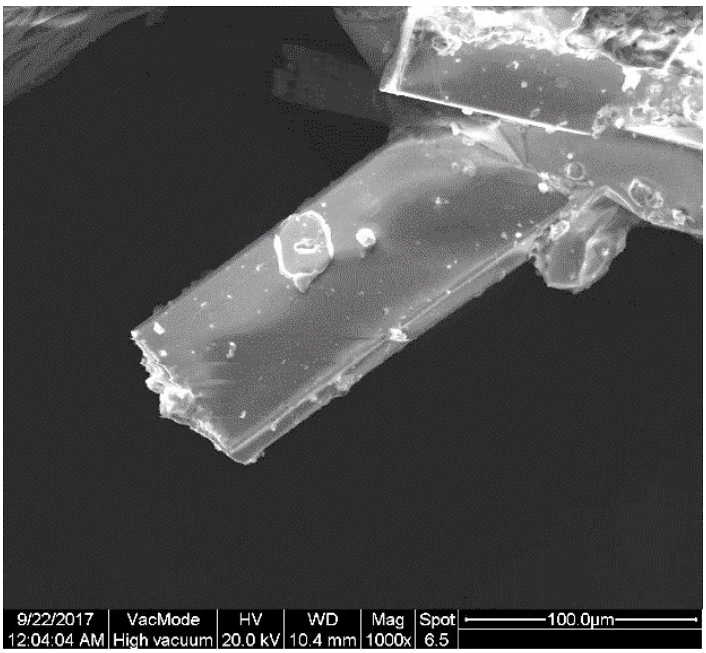

Fig S1. SEM image of $Sr_8Mg_7Si_9N_{22}$ crystals.

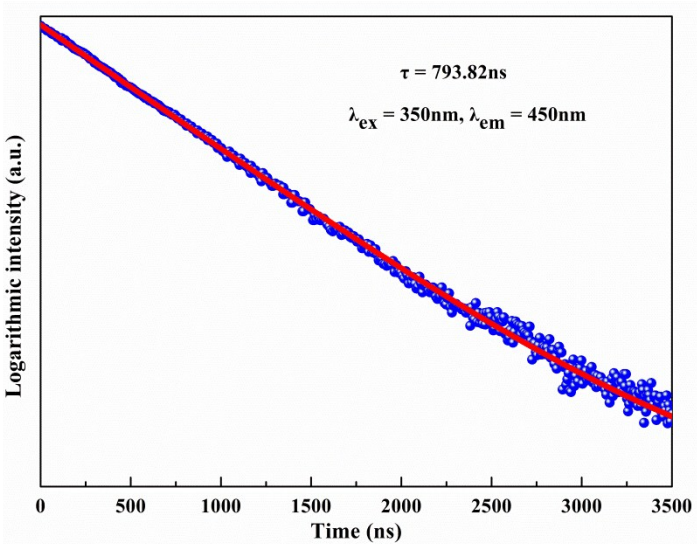

Fig S2. Observed (blue dot) and fitted (red line) decay curves of $Sr_{7.92}Mg_7Si_9N_{22}$:0.08Eu^{2+} by the excitation of 350 nm near-UV light.

Table S1. Crystallographic Data of $Sr_8Mg_7Si_9N_{22}$.

Formula	$Sr_8Mg_7Si_9N_{22}$
crystal system	Monoclinic
space group	*C* 2/m (No.12)
a (Å)	15.2798 (14)
b (Å)	7.4691 (7)
c (Å)	10.9358 (10)
β (°)	110.462 (3)
V (Å3)	1169.32 (19)
formula units per cell	Z = 2
density (g/cm^3)	4.068
F(000)	1336
diffractometer	Bruker D8 Quest
radiation	Mo Kα radiation, λ = 0.71073 Å
crystal size (mm^3)	0.10 × 0.04 × 0.03
color	clear light yellow
range in hkl	−18≤h≤17, −8≤ k≤8, −13 ≤l≤13
measured reflections	13538
independent reflections	1110
Absorption correction:	multi-scan
$\Delta\rho_{max}$, $\Delta\rho_{min}$ (e Å^{-3})	1.69, -1.50
R[$F^2 > 2\sigma(F^2)$] ,wR(F^2)	0.071, 0.169
S	1.04

Table S2. Atomic coordinates, occupancies, and isotropic atomic displacement parameters of $Sr_8Mg_7Si_9N_{22}$

Atom	x	y	z	Ueq(Å^3)	Occupancy
Sr1	0.0000	0.0000	0.0000	0.0371(5)	1
Sr2	0.2500	0.2500	0.5000	0.0320(5)	1
Sr3	0.0000	0.25119(15)	0.5000	0.0314(4)	1
Sr4	0.0000	0.5000	0.0000	0.0358(5)	1
Sr5	0.25283(8)	0.5000	0.01156(12)	0.0342(5)	1
Mg1	-0.0777(2)	0.2527(4)	0.1891(3)	0.0324(7)	1
Mg2	-0.1707(3)	0.5000	0.3182(4)	0.0323(10)	1
Mg3	0.0795(3)	0.0000	0.3193(4)	0.0387(10)	0.5
Si1	0.0711(3)	0.5000	0.3180(3)	0.0344(8)	1
Si2	0.0795(3)	0.0000	0.3193(4)	0.0387(10)	0.5
Si3	0.16860(18)	0.2348(4)	0.1747(2)	0.0364(7)	1
Si4	0.3386(3)	0.5000	0.3186(3)	0.0341(8)	1
N1	-0.0525(7)	0.5000	0.2852(9)	0.027(2)	1
N2	0.0904(6)	0.2900(13)	0.2471(8)	0.049(2)	1
N3	0.3663(7)	0.5000	0.4887(10)	0.035(2)	1
N4	0.1781(9)	0.0000	0.2150(12)	0.051(3)	1
N5	0.1280(5)	0.2531(9)	0.0115(6)	0.0321(18)	1
N6	0.1294(7)	0.5000	0.4880(10)	0.035(2)	1
N7	0.2830(6)	0.2906(13)	0.2481(8)	0.048(2)	1
N8	0.4436(7)	0.5000	0.2797(9)	0.028(2)	1

Table S3. Anisotropic displacement parameters /Å^2 of $Sr_8Mg_7Si_9N_{22}$.

Atom	U_{11}	U_{22}	U_{33}	U_{12}	U_{13}	U_{23}
Sr1	0.0329(9)	0.0312(10)	0.0474(11)	0.000	0.0143(8)	0.000
Sr2	0.0315(7)	0.0301(7)	0.0347(7)	0.0000(4)	0.0120(5)	-0.0004(4)
Sr3	0.0329(7)	0.0325(7)	0.0282(7)	0.000	0.0101(5)	0.000
Sr4	0.0327(9)	0.0300(10)	0.0465(10)	0.000	0.0159(8)	0.000
Sr5	0.0337(7)	0.0306(7)	0.0398(8)	0.000	0.0148(5)	0.000
Mg1	0.0376(17)	0.0321(18)	0.0258(15)	0.0003(12)	0.0090(12)	-0.0004(11)
Mg2	0.037(2)	0.034(2)	0.025(2)	0.000	0.0102(17)	0.000
Mg3	0.040(2)	0.040(2)	0.033(2)	0.000	0.0097(17)	0.000
Si1	0.0377(19)	0.033(2)	0.0300(18)	0.000	0.0084(15)	0.000
Si2	0.040(2)	0.040(2)	0.033(2)	0.000	0.0097(17)	0.000
Si3	0.0322(14)	0.0486(17)	0.0276(13)	-0.0001(11)	0.0094(11)	-0.0011(10)
Si4	0.0385(19)	0.035(2)	0.0285(17)	0.000	0.0111(15)	0.000
N1	0.034(5)	0.018(5)	0.028(5)	0.000	0.010(4)	0.000
N2	0.044(3)	0.058(3)	0.047(3)	-0.003(2)	0.019(2)	0.000(3)
N3	0.033(6)	0.031(6)	0.042(6)	0.000	0.016(5)	0.000
N4	0.051(7)	0.057(8)	0.043(7)	0.000	0.014(6)	0.000
N5	0.032(4)	0.033(5)	0.030(4)	-0.001(3)	0.010(3)	0.000(3)
N6	0.032(6)	0.032(6)	0.042(6)	0.000	0.015(5)	0.000
N7	0.043(3)	0.057(3)	0.046(3)	0.002(2)	0.017(2)	0.000(2)
N8	0.034(5)	0.020(5)	0.030(5)	0.000	0.011(4)	0.000